The anti-Müllerian hormone type II receptor: insights into the binding domains recognized by a monoclonal antibody and the natural ligand

Imed SALHI*†, Sylvie CAMBON-ROQUES*†, Isabelle LAMARRE‖, Daniel LAUNE‡, Franck MOLINA‡, Martine PUGNIÈRE‡, Didier POURQUIER§, Marian GUTOWSKI*†, Jean-Yves PICARD‖, Françoise XAVIER†‖, André PÈLEGRIN*† and Isabelle NAVARRO-TEULON*†[1]

*EMI 0227 INSERM/Université Montpellier I/CRLC Montpellier, Cancer Institute Val d'Aurelle – Paul Lamarque, 35 rue de la Croix Verte, 34298 Montpellier Cedex 5, France, †CNRS GDR 2352, Immunociblage des Tumeurs, 34298 Montpellier Cedex 5, France, ‡CPBS-CNRS UMR 5160, 34093 Montpellier Cedex 5, France, §CRLC Montpellier, Cancer Institute Val d'Aurelle – Paul Lamarque, 35 rue de la Croix Verte, 34298 Montpellier Cedex 5, France, and ‖Endocrinologie du Développement, INSERM U493, 92140 Clamart, France

Anti-Müllerian hormone (AMH) [also called Müllerian inhibiting substance (MIS)] is a member of the transforming growth factor-β family. AMH and its type II receptor (AMHR-II) are involved in the regression of the Müllerian ducts in the male embryo, and in gonadal functions in the adult. AMH is also known to be a marker of granulosa and Sertoli cell tumours. We selected a high-affinity monoclonal antibody, mAb 12G4, specific for human AMHR-II (hAMHR-II), by FACS analysis, Western blotting and immunohistochemical staining of a hAMHR-II-transfected CHO (Chinese hamster ovary) cell line, normal adult testicular tissue and granulosa cell tumours. Using peptide array screening, we identified the binding sequences of mAb 12G4 and AMH on the receptor. Identification of Asp^{53} and Ala^{55} as critical residues in the DRAQVEM minimal epitopic sequence of mAb 12G4 definitively accounted for the lack of cross-reactivity with the murine receptor, in which there is a glycine residue in place of an aspartic acid residue. In a structural model, the AMH-binding interface was mapped to the concave side of hAMHR-II, whereas the mAb 12G4-binding site was located on the convex side. mAb 12G4, the first mAb to be raised against hAMHR-II, therefore has unique properties that could make it a valuable tool for the immunotargeting of tumours expressing this receptor.

Key words: anti-Müllerian hormone (AMH), AMH type II receptor (AMHR-II), peptide array, structure modelling.

INTRODUCTION

Anti-Müllerian hormone (AMH) is a member of the TGF-β (transforming growth factor-β) family of growth factors. In contrast with other members of the family, which are widely expressed, AMH is expressed in a highly tissue-specific manner, restricted to Sertoli cells of the testis and granulosa cells of the ovary [1–3]. The most striking effect of AMH is to induce the regression of the Müllerian ducts, which, in females, differentiate into the uterus, Fallopian tubes and upper vagina [4]. Female transgenic mice overexpressing the human AMH gene lack a uterus, oviducts and sometimes ovaries [5], whereas in male homozygote AMH-deficient mice, Müllerian ducts do not regress [6]. AMH has a negative effect upon steroidogenesis and germ-cell development (reviewed in [7,8]). Breast, prostate and ovarian cancer cells have also been proposed as targets of AMH action [8,9], and the inhibitory effect of the hormone has been shown *in vitro* [10] and *in vivo* [11,12]. AMH has also been described as a potent marker of recurrence of GCTs (granulosa cell tumours) and Sertoli cell tumours [13,14].

The AMHR-II (AMH type II receptor) gene has been isolated in the rat [15], rabbit [16], human (hAMHR-II) [17] and mouse (mAMHR-II) [6]. It contains 11 exons: exons 1–3 code for the extracellular domain, composed of 127 amino acids in the human receptor, and exon 4 codes for the transmembrane domain, composed of 26 amino acids. The predicted sequence of AMHR-II shares an overall similarity of approx. 30 % with other type II receptors of the TGF-β family. Exon 2 seems to be essential for ligand binding, as shown in the rabbit receptor [16]. As a member of the TGF-β family, AMH is thought to exert its effects through two distinct membrane receptors, type II (i.e. AMHR-II) and type I, and thus AMHR-II must be co-expressed with an appropriate type I receptor for signal transduction. In spite of many efforts devoted to the identification of an AMH-specific type I receptor, the identity of the type I receptor remains controversial. Three BMP (bone morphogenetic protein) type I receptors have been considered: ALK6 (activin receptor-like kinase 6) [18], ALK2 [19] and ALK3 [20]. Upon ligand binding, the type II receptor recruits and phosphorylates the type I receptor, which initiates subsequent downstream activation of a set of cytoplasmic effector proteins: Smads 1, 5 and 8 [18,19,21]. Other signalling pathways involving β-catenin [22] and NFκB (nuclear factor κB) [9,23] have also been described.

AMHR-II is specifically expressed in the natural tissue targets, the reproductive organs and the gonads. In the Müllerian duct, where AMH induces regression by a paracrine mechanism, AMHR-II is expressed in the mesenchyme [24]. In the male rat embryo, the cranial-to-caudal pattern of mesenchymal expression of AMHR-II protein is correlated with the cranio-caudal pattern of the epithelium regression [22]. Mutations in AMHR-II or AMH cause male sexual abnormalities, e.g. pseudohermaphroditism in male transgenic mice [6] {known as persistent Müllerian duct syndrome (PMDS) in humans [25]}. In the female, AMHR-II expression is maintained along the length of the Müllerian duct, and is detected in the normal and gravid uterus [26]. Female AMHR-II- or AMH-deficient mice are normal and as fertile

Abbreviations used: AMH, anti-Müllerian hormone; AMHR-II, AMH type II receptor; (h/m)AMHR-II, (human/mouse) AMHR-II; ECD-AMHR-II, extracellular domain of AMHR-II; BMP, bone morphogenetic protein; CHO, Chinese hamster ovary; FCS, fetal-calf serum; GCT, granulosa cell tumour; mAb, monoclonal antibody; RAMFc, rabbit anti-mouse Fc antibody; RT, reverse transcriptase; SPR, surface plasmon resonance; TGF-β, transforming growth factor-β.

[1] To whom correspondence should be addressed (e-mail iteulon@valdorel.fnclcc.fr).

as young adults. AMH and AMHR-II are co-expressed in the testicular Sertoli and ovarian granulosa cells, and in derived cells, such as Smat-1 [27] and AT29C [28], respectively. Expression of AMHR-II alone has been detected in Leydig cells of rodents [29,30] and in cells of humans [10], but not in murine ovarian surface epithelium [16, 31].

In spite of the growing interest in AMHR-II with respect to development and cancer, few tools for diagnosis or therapy have been developed. Here, we report the selection of a high-affinity mAb (monoclonal antibody) that efficiently detected the receptor in human tissues. To investigate the binding of AMH and mAb 12G4 to the AMHR-II at a molecular level, we performed a fine analysis of their different binding sites and provide a structural model.

EXPERIMENTAL

Cell culture and tissues

CHO-3W, a stably AMHR-II cDNA-transfected CHO (Chinese hamster ovary) cell line, was kindly provided by Dr N. Di Clemente (INSERM U493, Clamart, France). The CHO-3W cell line was grown as described previously [17]. Untransfected CHO cells were cultured in RPMI 1640 medium containing 10 % (v/v) FCS (fetal-calf serum), 100 units/ml penicillin and 100 μg/ml streptomycin. AT29C, a mouse granulosa cancer cell line [28], was cultured in Dulbecco's modified Eagle's medium (Life Technologies) containing 10 % FCS and penicillin/streptomycin at the above concentrations. Cultures were grown at 37 °C in a humidified atmosphere of 5 % CO_2. Frozen human testicular tissue was provided by Dr Philippe Durand (INSERM U418, Hôpital Debrousse, Lyon, France).

Generation of mAbs

The recombinant extracellular domain of human AMHR-II (ECD-hAMHR-II), expressed in bacteria and purified as a His_6-tag fusion protein [18], was used as an immunogen. Mice hybridomas were generated by immunizing BALB/c mice four times subcutaneously at 2–3-week intervals with 20 μg of protein in complete Freund's adjuvant (Sigma) for the first injection, and incomplete Freund's adjuvant (Sigma) for subsequent injections. An intravenous booster injection of ECD-hAMHR-II was given 3 weeks after the fourth immunization. After a further 3 days, spleen cells from immunized mice were fused with the mouse myeloma cell line P3-X63-Ag.8.653. Supernatants from newly generated clones were screened by ELISA using ECD-hAMHR-II. The specificity for hAMHR-II of supernatants was confirmed by FACS on CHO-3W and AT29C cells. Selected mAbs were purified on a Protein A–Sepharose column (Amersham Biosciences).

ELISA

Specificity of the mAbs was evaluated by ELISA. Briefly, ECD-hAMHR-II was immobilized on to a Maxisorp plate (Nunc) at a concentration of 1 μg/ml in 50 mM Na_2CO_3, pH 9.0, and blocked with PBS containing 10 g/l BSA. Binding of the antibodies was detected by a horseradish-peroxidase-conjugated anti-mouse IgG (Silenus Laboratories, Melbourne, Vic., Australia). The plates were developed using OPD (*o*-phenylenediamine) as substrate, according to the manufacturer's instructions (Sigma).

Western blotting

RIPA [50 mM Tris/HCl (pH 7.4)/150 mM NaCl/1 % deoxycholate/1 % Nonidet P40/2 mM EDTA/0.1 % SDS/1 mM PMSF] lysates of cultured cells or recombinant proteins were resolved by SDS/PAGE, using 10 % (w/v) polyacrylamide Tris/glycine gels under reducing conditions (5 % 2-mercaptoethanol). Proteins were blotted on to PVDF membranes (Immobilon-P; Millipore) and incubated with mAb 12G4 (5 μg/ml). Specific binding was detected using a horseradish-peroxidase-conjugated anti-mouse IgG (Silenus), and visualized by using enhanced chemiluminescent detection (ECL Detection Reagents; Amersham Biosciences). The Mark 12 molecular-mass marker was purchased from Invitrogen.

Surface plasmon resonance (SPR)

SPR experiments were performed at 25 °C by using a Biacore 3000 instrument (Biacore AB, Stevenage, Herts., U.K.). An RAMFc (rabbit anti-mouse Fc) antibody was immobilized on a CM5 sensor chip via primary amino groups, according to the manufacturer's instructions. For affinity determination, mAb 12G4 (166 nM) was first injected, and then hAMHR-II at various concentrations was injected simultaneously into the measuring and control (no protein immobilized) flow cells at a flow rate of 30 μl/min. The running buffer was HBS [10 mM Hepes (pH 7.4)/150 mM NaCl/3 mM EDTA/0.005 % P20 detergent], and regeneration of the flow cells was performed using 12 μl of HCl (50 mM). To evaluate the affinity of purified recombinant plasmin-cleaved AMH for hAMHR-II presented by mAb 12G4, the injection of the mAb on the RAMFc was followed by an injection of ECD-AMHR-II alone followed by an injection of cleaved AMH. All the sensorgrams were corrected by subtracting the low signal of the control flow cell and the dissociation curve of mAb 12G4. Experiments at different flow rates showed an absence of mass transport and rebinding effects. The data were globally fitted to a 1:1 Langmuir model using Bia-Evaluation 3.2 software. Antibody isotyping was performed using a mouse antibody subclass kit (Biacore AB).

Flow cytometry

Cells were resuspended in ice-cold staining buffer (PBS/1 % BSA/0.1 % sodium azide), and incubated on ice for 45 min with mAb 12G4 (20 μg/ml). Cells were washed with ice-cold staining buffer, pelleted by centrifugation at 4 °C, and then incubated for 45 min in the dark with a goat anti-mouse IgG–FITC conjugate (Silenus). For analysis of AMH binding, cells were incubated with human AMH (20 μg/ml) for 45 min. After washing, cells were incubated with 20 μg/ml of M10.6, a murine monoclonal antibody raised against human recombinant AMH and directed against a species-specific epitope at the N-terminus of the molecule [32]. Because of a specific and stable reassociation of the N- and C-terminal fragments of the plasmin-cleaved protein [33], the M10.6 antibody could be used to detect AMH binding to its receptor. Detection of antibody binding was performed as described above. For competitive FACS analysis, CHO-3W cells were incubated at 4 °C for 45 min with mAb 12G4 at a concentration of 2 μg/ml. After washing, cells were incubated with increasing concentrations (2, 20 and 200 μg/ml) of recombinant plasmin-cleaved AMH. mAb binding was revealed using a goat anti-mouse IgG–FITC conjugate (Silenus). In all experiments, after the final wash, the cells were pelleted and resuspended in PBS. The mean relative fluorescence after excitation at a wavelength of 488 nm

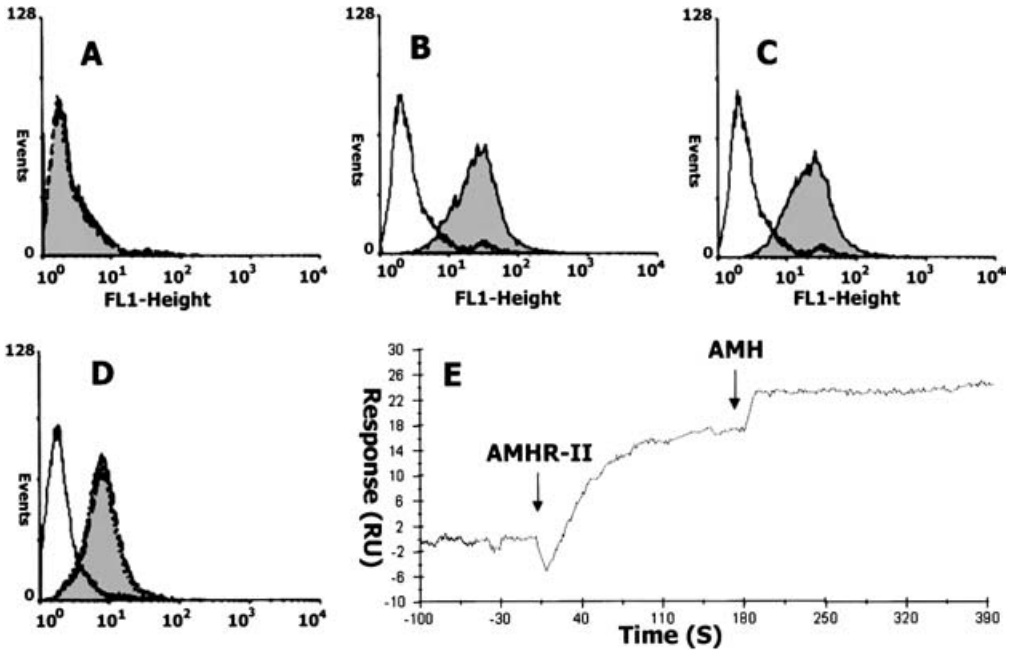

Figure 1 Flow cytometric analysis of cleaved AMH and mAb 12G4 binding on live, non-permeabilized cells

Detection of mAb 12G4 binding on the cell surface was performed using an FITC-conjugated anti-mouse antibody. Detection of AMH binding was performed using a mixture of anti-AMH mAb M10.6 and FITC-conjugated anti-mouse antibody. Controls were treated only with FACS buffer and the FITC conjugate. (**A**) Neither mAb 12G4 nor AMH was able to bind the untransfected CHO cell line: the histograms obtained are superimposed on to the control. Both mAb 12G4 (**B**) and AMH (**C**) stain the hAMHR-II-expressing CHO-3W cell line. Competition between AMH and mAb 12G4 for binding on CHO-3W cells was performed by FACS analysis as described in the Experimental section. (**D**) When AMH was used as the competitor, no shift of the histogram plots was observed at either 2, 20 or 200 μg/ml of AMH. (**E**) AMH is able to bind hAMHR-II immobilized on mAb 12G4 as shown in a Biacore assay where hAMHR-II was injected on the RAMFc-bound mAb 12G4 followed by injection of AMH. In a control experiment, no binding of AMH on the RAMFc-bound mAb 12G4 was observed (results not shown).

was determined for each sample on a FACScan flow cytometer (Becton–Dickenson) and immediately analysed with Cell-Quest software (Becton–Dickenson).

RNA extraction and analysis

For detection of AMHR-II mRNA expression, total RNA of cells and tissues was prepared using the RNeasy kit (Qiagen). RNA quality was analysed using the RNA 6000 Nano Labchip Kit (Agilent, Palo Alto, CA, U.S.A.). RT (reverse transcriptase)-PCR was performed using the SuperScript First-Strand Synthesis System (Invitrogen). Quantitative PCR analysis was performed using the LightCycler-FastStart DNA Master SYBR Green I kit (Roche Molecular Biochemicals) with the following oligonucleotides: forward primer, 5′-GGGAAGGAGGTCATGCAG-TG-3′; and reverse primer, 5′-CTCAGCTTGGAACTGAGCC-AC-3′.

SPOT peptide synthesis, probing and regeneration

Two arrays of overlapping 15-mer peptides corresponding to the extracellular domains of hAMHR-II and mAMHR-II were prepared as described previously [34]. To avoid possible disulphide-bond formation, cysteine residues were replaced with serine. After an overnight saturation step in blocking buffer (Genosys), mAb 12G4 was added to the membrane (1 μg/ml; 90 min incubation at 37 °C). After three washes in TBS/Tween-20 (0.1 %), a 1:5000 dilution of a horseradish-peroxidase-conjugated anti-mouse IgG (Silenus) was added and incubated for 1 h at room temperature ($\approx$21–22 °C). Bound antibody was detected by enhanced chemiluminescence (ECL Detection Reagents, Amersham). To allow the re-use of the membrane, it was sequentially treated with reagent A (8 M urea with 1 % SDS and 0.1 % 2-mercaptoethanol), reagent B (ethanol/water/acetic acid; 5:4:1, by vol.), and methanol (three washes of 10 min for each buffer), to remove the molecules bound to the peptides.

Modelling and structural analyses

The structure of the ECD-hAMHR-II was modelled using the homology-modelling approach. The templates used were X-ray structures of mouse, rat and human extracellular domains of activin receptor (Protein Data Bank accession nos. 1BTE, 1NYS and 1XLS respectively). The disulphide-bridge pattern was deduced from three-dimensional structure analysis of the templates compared with the hAMHR-II sequence. After multiple sequence alignments and structural superimpositions using COMPARER software [35], structural alignments were derived using JOY 4.0 software [36]. This final alignment was used for homology modelling using a modeller package [37]. Refined structures were evaluated with PROSA II [38], analysed and displayed using SPDBV 7.2 [39]. Solvent-accessible surfaces were calculated using SPDBV 7.2.

Immunohistochemistry

Routinely fixed, paraffin-embedded, 3 μm-thick tissue sections were de-paraffinized, rehydrated and then immersed in a 95 °C water bath, either in citrate buffer, pH 6.0, for cell lines or in target retrieval solution, pH 9.9 (DakoCytomation, Carpinteria, CA, U.S.A.) for tissue sections. Subsequently, tissue sections were first incubated with mAb 12G4 as the primary antibody, and then processed for immunohistochemistry on the Autostainer

S3400 System (DakoCytomation), with either the LSAB kit (DakoCytomation) for the cell lines or Envision (DakoCytomation) for tissue sections, according to the protocols recommended by the manufacturer. Specificity of staining was confirmed by replacing the primary antibody with an isotype-matched irrelevant IgG at the same concentration.

RESULTS

Selected mAb 12G4 specifically binds to hAMHR-II

Hybridomas were established from BALB/c mice immunized with purified recombinant ECD-hAMHR-II. To select a mAb specific for hAMHR-II, screening was performed by ELISA using ECD-hAMHR-II and ECD-mAMHR-II. Only one clone, 12G4, positive for hAMHR-II and negative for mAMHR-II, was selected. This specificity was confirmed by FACS analysis for the binding of mAb 12G4 (Figure 1B) and cleaved human AMH (Figure 1C) to the hAMHR-II-expressing CHO-3W cell line. In the untransfected CHO control cell line, no immunoreactivity was observed with either mAb 12G4 or AMH (Figure 1A). The murine granulosa cell line AT29C, which expresses mAMHR-II as confirmed by FACS analysis using a rabbit polyclonal antibody recognizing both human and murine receptors, was unable to bind mAb 12G4 (results not shown). These results confirmed the specificity of mAb 12G4 for hAMHR-II. In Western-blotting assays, mAb 12G4 was tested with lysates from the CHO-3W, CHO and AT29C cell lines, and a normal adult testicular tissue. mAb 12G4 detected an approx. 66 kDa band corresponding to hAMHR-II in the CHO-3W cells (Figure 2A, lane 1) and in testicular tissue (Figure 2A, lane 4), and a 15 kDa band corresponding to the recombinant ECD-hAMHR-II (Figure 2A, lane 5). Furthermore, mAb 12G4 did not recognize the murine receptor expressed either in the mouse AT29C cell line or in its recombinant form (Figure 2A, lanes 3 and 6). To confirm these findings, hAMHR-II mRNA expression was analysed using the sensitive Lightcycler quantitative-PCR technique. The mRNA was found in CHO-3W cells and in the testicular tissue, but not in the CHO cell line (Figure 2B).

We measured the kinetic parameters and affinity constant of mAb 12G4 to the ECD-hAMHR-II by Biacore technology (results not shown). The 5.54×10^3 $M^{-1} \cdot s^{-1}$ association rate constant, and the very low dissociation rate, which was close to the limit of the technique (5×10^{-6} s^{-1}), led to a K_d value of at least 0.86×10^{-9} M. Isotyping using Biacore analysis revealed that mAb 12G4 is an IgG1-type immunoglobulin.

AMH-binding site on hAMHR-II is unaffected by mAb 12G4

The relative binding of mAb 12G4 and AMH on hAMHR-II was analysed by FACS by measuring the ability of mAb 12G4 to still bind hAMHR-II on CHO-3W cells when AMH was added at a 1-, 10- or 100-molar excess, corresponding to 2, 20 or 200 μg/ml of AMH respectively (Figure 1D). The histograms obtained at these three concentrations of AMH are identical with that obtained without AMH (shown by the filled histogram), showing that AMH was unable to displace bound mAb (Figure 1D). Moreover, it was shown by Biacore analysis that mAb 12G4 did not inhibit the binding of AMH to the ECD-hAMHR-II (Figure 1E). The K_d of AMH for ECD-hAMHR-II bound by the mAb 12G4 was in the range of 10^{-9} M, as published previously [17]. No binding of AMH by the mAb 12G4 was observed in the absence of the ECD-hAMHR-II. Therefore we can conclude that mAb 12G4 and AMH bind to non-overlapping epitopes on hAMHR-II.

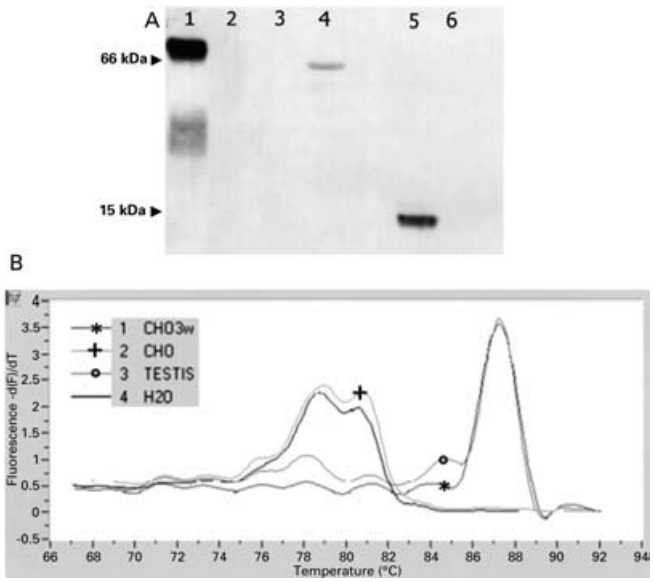

Figure 2 AMHR-II detection using mAb 12G4 by Western blotting (A), and melting curves for RT-PCR products obtained in a representative experiment with amplification of the AMHR-II transcript (B)

(**A**) A Western blot is shown, illustrating AMHR-II detection using mAb 12G4. Cell lysates were prepared as described in the Experimental section. Samples of total proteins for cell lines (20 μg), testicular tissue (50 μg) and recombinant human and murine extracellular domains (10 ng) were loaded on to an SDS/10 % polyacrylamide gel. hAMHR-II was detected in the CHO-3W cell line (lane 1) and in the adult testicular tissue (lane 4) as a band of approx. 66 kDa, and the recombinant extracellular domain as a band of approx. 15 kDa (lane 5). No bands were detected in the untransfected CHO cell line (lane 2), in the murine granulosa cell line AT29C (lane 3), or in the recombinant murine extracellular domain (lane 6). (**B**) Melting curves are shown for RT-PCR products obtained in a representative experiment with amplification of the AMHR-II transcript. Peaks were obtained at the melting temperatures by plotting the negative derivative of the fluorescence signal with respect to temperature against temperature [$-(dF/dT)$ versus T]. The reaction products of CHO-3W and testis extracts show only one sharp peak at $T_m = 87$ °C, indicating that only one cDNA was amplified. In the negative controls (water and CHO), a double peak at approx. 80 °C corresponds to primer dimerization.

Asp[53] and Ala[55] are the major contributor residues in the minimal epitopic sequence recognized by mAb 12G4

Over the past decade, SPOT peptide arrays have become a widespread and powerful tool to study molecular recognition events and to identify biologically active peptides. This simple, flexible and time-saving technique has a variety of applications, such as antibody epitope mapping and the study of protein–protein, enzyme–substrate or enzyme–inhibitor interactions.

SPOT technology was used to map and characterize the mAb 12G4 epitope on hAMHR-II. A set of overlapping 15-mer peptides that were frame-shifted by one residue each, spanning the entire ECD-hAMHR-II and ECD-mAMHR-II, was synthesized on a cellulose membrane, and then the binding of the mAb 12G4 to these peptides was evaluated. No binding was detected with any peptide from the murine receptor sequence (results not shown), confirming the specificity of mAb 12G4 for hAMHR-II. The recognition pattern observed for mAb 12G4 on hAMHR-II is shown in Figure 3(A). Antibody bound to peptides 45–53, but not to the preceding or following ones. Therefore the minimal epitopic sequence of mAb 12G4 could be mapped to residues DRAQVEM, which are common to the nine reactive peptides (Figure 3B). Interestingly, although mAb 12G4 specifically recognized the human receptor, the alignment of the hAMHR-II and mAMHR-II sequences showed that within

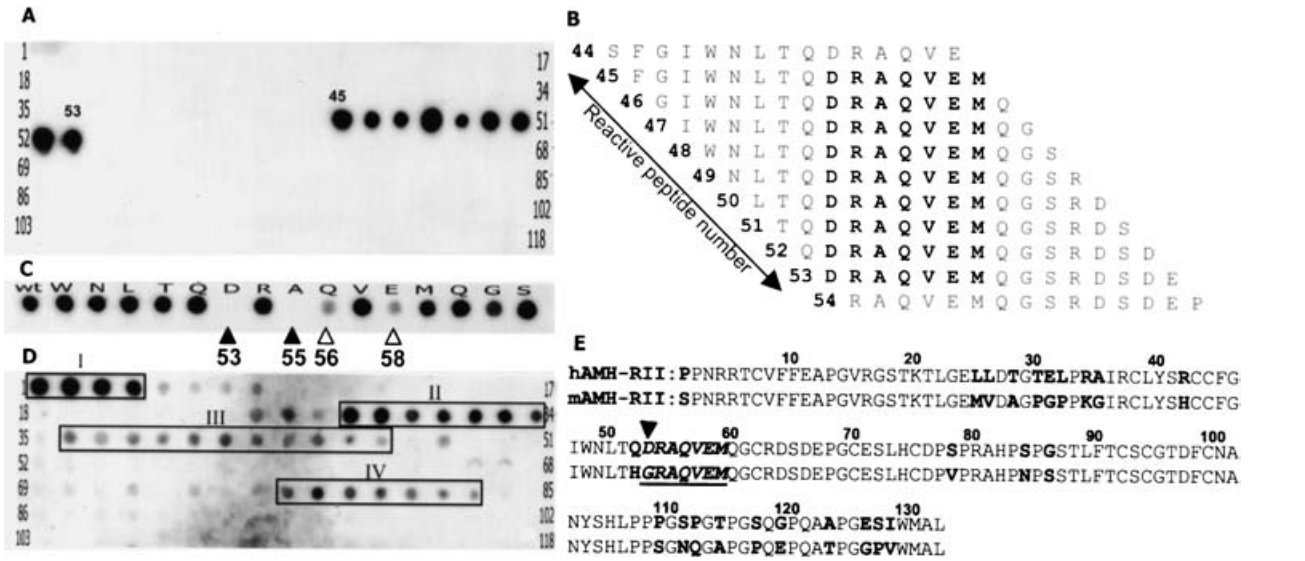

Figure 3 Mapping epitopes of mAb 12G4 and AMH on the hAMHR-II sequence using SPOT technology

Analysis of the reactivity of a set of cellulose-bound peptides representing the extracellular domain sequences of hAMHR-II in the form of overlapping 15-mer peptides (one-residue frameshift; the structures are shown in **B**). The numbers in (**A**), (**B**) and (**D**) correspond to peptide identification on the cellulose membrane. (**A**) Reactivity with 1 μg/ml mAb 12G4 was detected by horseradish-peroxidase-conjugated anti-mouse IgG. (**B**) The identified epitope (DRAQVEM) is the common sequence of immunoreactive peptides (shown by the residues numbered 45–53). (**C**) Determination of residues contributing to the binding of mAb 12G4 by alanine scanning. Each residue of the immunoreactive peptide 48 (wt) was successively replaced by an alanine; a contribution by alanine was determined by its replacement by a glycine residue. The membrane was probed with 100 ng/ml mAb 12G4. Amino acid residues Asp^{53} and Ala^{55} (black arrowheads) appear to be critical for mAb 12G4 binding, since their replacement completely abolished the reactivity. Replacement of Gln^{56} and Glu^{58} (white arrowheads) gave a significantly lower signal intensity. (**D**) Recombinant hAMH binding site mapping on the hAMHR-II sequence was performed at a concentration of 5 μg/ml; reactivity was detected using the anti-AMH mAb M10.6 and the horseradish-peroxidase-conjugated anti-mouse IgG. The four reactive groups (I to IV) are boxed. (**E**) Alignment of the human and murine receptor sequences. The Asp^{53} residue (arrowhead) in the human receptor sequence is replaced by a Gly^{53} in the murine receptor; the epitopic sequence is underlined.

the minimal epitopic sequence only one residue is different (Figure 3E).

The contribution to antibody binding of each residue in the epitopic sequence was assessed by preparing a series of alanine analogues of peptide 48. All residues were replaced in turn by alanine; the alanine residue (Ala^{55}) was replaced by a glycine (Figure 3C). Substitution of the aspartic acid (Asp^{53}) and alanine (Ala^{55}) residues completely abolished the binding of mAb 12G4, suggesting that these residues are essential for the interaction. This result explains why mAMHR-II, in which the single difference in the epitopic sequence is a glycine (Gly^{53}) in place of the aspartic acid (Asp^{53}), is not recognized by mAb 12G4. A decrease in spot signal intensity was observed when the glutamine (Gln^{56}) and glutamic acid (Glu^{58}) residues were replaced by an alanine (Figure 3C), indicating that these two residues also participate, albeit to a lesser extent, in antibody recognition.

AMH binding site mapping

We used the hAMHR-II SPOT array, as described above, to determine the binding site of AMH on its receptor. AMH binding was revealed by using the M10.6 anti-AMH mAb (Figure 3D). Four groups of peptides were reactive with the hormone: group I (peptides 1–4), group II (peptides 28–34), group III (peptides 36–46) and group IV (peptides 77–83). These groups correspond, respectively, to these four peptides: RRTCVFFEAPGV, RAIRCLYSR, GIWNL and PSPGSTLFT. The same reactivity was detected with the murine receptor in which peptides in groups I and III are conserved, and those in groups II and IV are very similar. However, when AMH was used at a lower concentration (2 μg/ml), groups I and II were still strongly reactive, whereas the reactivity of groups III and group IV was very weak (results not shown).

The binding sites of AMH and mAb 12G4 are independently located on hAMHR-II

Different type II receptor structures were determined, free or bound to their ligands. The overall structure consists of a cysteine 'knot', stabilizing a three-finger toxin fold.

Homology modelling of hAMHR-II resulted in a three finger domain (three β-hairpin loops; Figure 4A). Compared with the activin receptors, the first N-terminal loop (finger 1) was found to be longer in hAMHR-II. As in the activin receptors used as templates [40], the core of the structural domain was maintained by five disulphide bridges in close vicinity, but the connectivity is different: C7–C44, C38–62, C43–70, C75–C92 and C94–C99 (Figure 4C). The solvent-accessible surface of hAMHR-II was globally negatively charged (Figure 4B).

The minimal epitopic sequence (Asp^{53}–Met^{59}) of mAb 12G4 was exposed to the solvent at the extremity of finger 2. It is interesting to note that the main residues contributing to mAb 12G4 binding on hAMHR-II (Asp^{53} and Ala^{55}) belong to the β-turn of the central long loop, which is located on the convex side of the receptor (Figure 4D).

Considering the interaction of AMH with its receptor, two groups of peptides from hAMHR-II were shown by SPOT technology to react strongly, and a third (group IV) to a minor extent. Regions I and II, corresponding to residues 4–15 and 34–42 respectively, were both located on the two β strands of finger 1 at the N-terminus of hAMHR-II (Figure 4A). Region IV, corresponding to residues 83–91, was mapped to the finger 3 loop.

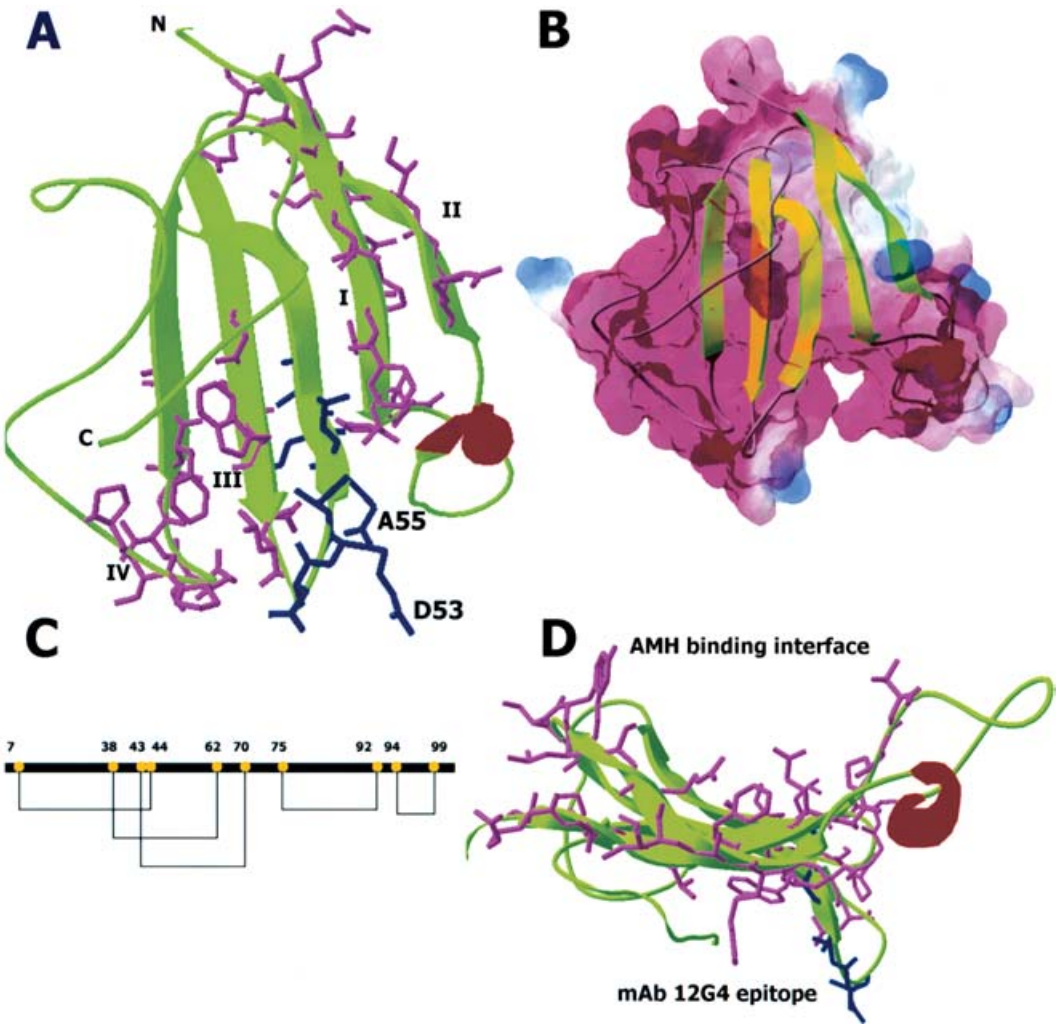

Figure 4 hAMHR-II three-dimensional model

(**A**) hAMHR-II ribbon representation with secondary structures: the four regions reactive with AMH are represented in pink, and are numbered I–IV (refer to the legend for Figure 3C). The epitope of mAb 12G4 is represented in blue and the two major contributor residues Asp^{53} and Ala^{55} are labelled. The bright-red structure shown in the right-hand part of (**A**) [and also in (**D**)] represents the α-helix of finger 1 of the receptor. (**B**) The calculated solvent-accessible surface of hAMHR-II with the same orientation as in (**A**). (**C**) For clarity, the cysteines involved in disulphide bridges are represented schematically (in yellow) with their connectivity shown by the adjoining lines, and are numbered with reference to the sequence in Figure 3. Electrostatic potentials are represented by a colour scale from − 1.8 (red) to 1.9 (blue). (**D**) Top view of the AMHR-II model, showing the concave (up) and the convex (down) sides; the mAb 12G4 epitope (in blue) is located on the convex side, and the major parts of the residues reactive with AMH (shown in pink) are located on the concave side.

Thus the accessible surface of AMHR-II, located on the concave side, appears to constitute a binding interface between AMH and hAMHR-II (Figure 4D).

AMHR-II is detected in human GCTs, Sertoli and Leydig cells

Immunohistochemical analysis has shown that mAb 12G4 is able to detect hAMHR-II in relevant target tissues, using CHO and CHO-3W cell lines as the control. As expected, strong staining was observed in CHO-3W cells expressing hAMHR-II, whereas CHO cells were not stained (Figure 5A). Interestingly, in the human adult testis, AMHR-II was detected not only in Sertoli cells, but also in Leydig cells (Figure 5B). Immunohistochemistry performed on a primary GCT section showed that granulosa cells exhibited strong staining, whereas the fibromatous tissue was not stained (Figure 5C). In a section of a recurrent GCT localized in the mesentery, immunoreactivity was also intense and homogeneous (Figure 5D).

DISCUSSION

During development, AMHR-II has a temporal and space-dependent function in Müllerian-duct regression, and AMHR-II is expressed exclusively in the gonads and reproductive organs, where the hormone exerts its biological effects.

Despite the fact that AMHR-II was cloned in 1994, the tools used for its detection are today limited to the analysis of its mRNA expression, or to identification of the protein using polyclonal antibodies. In the present study, we demonstrated by Western blotting and by FACS that the first mAb specifically directed to hAMHR-II, IgG1 mAb 12G4, is able to bind the receptor without inhibiting AMH binding. Using SPOT array technology, we identified the sequence DRAQVEM as the minimal epitopic sequence of this high-affinity mAb. We also mapped the AMH-binding site on hAMHR-II. Our results allowed us to provide a molecular model detailing the binding of mAb 12G4 and AMH on the extracellular domain of the human receptor. Furthermore,

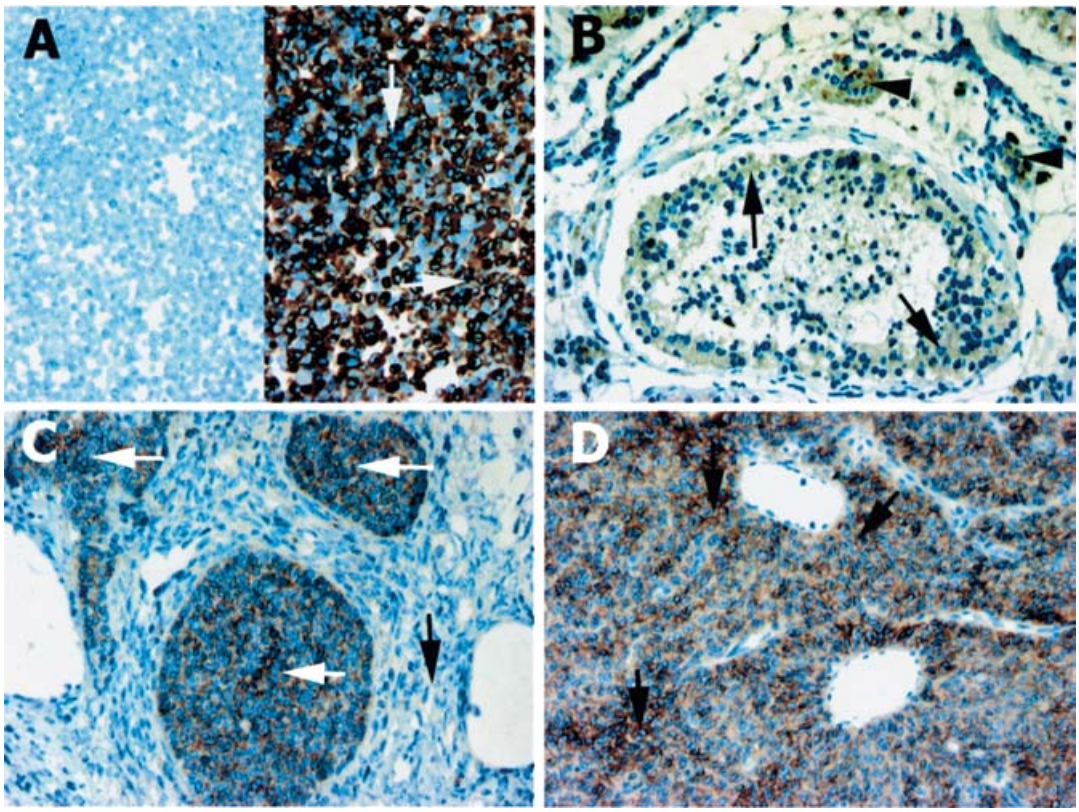

Figure 5 Immunohistochemical staining (brown) of AMHR-II with mAb 12G4

AMHR-II immunoreactivity was detected in: (**A**) CHO-3W cells permanently expressing hAMHR-II (shown by the arrows in the right panel), but not in control CHO cells (left panel); (**B**) Sertoli cells (arrows) and Leydig cells (arrowheads) of a frozen adult human testis section; (**C**) granulosa cells (white arrows) of a 52-year-old woman diagnosed with a stage IIIB GCT on the right ovary measured to be 16 cm: fibromatous tissue was not stained (black arrows); (**D**) granulosa cells of a 59-year-old woman diagnosed with a GCT on the left ovary in 1982, recurrence in 2001: a tumour was localized in the mesentery. Sections were stained with mAb 12G4 as described in the Experimental section. For CHO-3W and CHO staining, mAb 12G4 was used at a concentration of 10 μg/ml; for tissue section staining it was used at a concentration of 30 μg/ml. No staining was confirmed by replacing mAb 12G4 with an irrelevant murine IgG at the same concentration.

immunohistochemical analysis demonstrated that mAb 12G4 specifically detects the receptor in relevant target human tissues.

The results of the binding activity of synthetic peptides derived from the primary structure of AMHR-II demonstrated that mAb 12G4 is able to discriminate between two sequences differing by only one residue. The DRAQVEM minimal epitopic sequence, characterized on hAMHR-II, differs from the mAMHR-II primary structure only by an aspartic acid residue (Asp^{53}) being replaced by glycine (Gly^{53}). Alanine scanning results demonstrated that Asp^{53} is essential for recognition and for the specificity of mAb 12G4 for hAMHR-II. Interestingly, the epitope recognized by mAb 12G4 is located in a region that is not fully conserved in the sequence of the other receptors belonging to the TGF-β family, as shown by sequence alignment. Considering the molecular model provided and the electronic potential at the surface of each protein, the human receptor seems to be locally more negatively charged due to the presence of the Asp^{53} residue instead of Gly^{53}. Indeed, Asp^{53} in the human receptor is one of the major contributors to the mAb 12G4 epitope, and is probably responsible for the mAb 12G4 specificity for the human receptor, due to a local shift in electrostatic potential.

Peptide array screening allowed us to map four reactive regions, which probably constitute the potential binding interface between AMH and its receptor. These peptides are characterized by their high content of hydrophobic residues, which generally contribute towards binding interfaces. These binding sequences are located on the concave side of AMHR-II, and they are different from those of TGF-β3, mapped to finger 1 in TGF-βRII [41], activin A, mapped to the core of the concave side of ActRIIB [42], and BMP7, mapped to the core of ActRII [43]. Our results support the hypothesis that each TGF-β member has a distinct binding interface [43]. Furthermore, it has been demonstrated that, in the rabbit, exon 2 seems to be essential for ligand binding [16]. Interestingly, the amino acid residues 4–15 and 34–42 characterized in the present study are coded by exon 2 on the human gene.

All the structural and modelling data show that mAb 12G4 and AMH-binding sites are independently located on hAMHR-II. Indeed, the mAb 12G4-binding site was mapped to the convex side of AMHR-II, and the AMH-binding site to the concave side, confirming our previous results obtained by Biacore and FACS experiments.

Until 1990, AMH expression was thought to be restricted to Sertoli cells of the fetal and adult testes, and granulosa cells of the postnatal ovary. It was subsequently postulated by experiments on male transgenic mice overexpressing the human AMH gene that high levels of AMH could influence the function of Leydig cells [5]. Indeed, in adult male mice, AMHR-II expression was detected in Leydig cells, suggesting that AMH exerts its effect on these cells directly via its receptor [29,44]. In the present study, we show for the first time, by immunohistochemical studies using mAb 12G4, the presence of the AMHR-II protein on Leydig cells in human testicular tissue (Figure 5B), confirming in humans results reported previously [45].

GCTs are neoplasms that produce steroids and peptide hormones, such as inhibin and AMH, which are used as biochemical markers [13,46,47]. A powerful and easy to perform ELISA for AMH determination is now available, which allows the evaluation of the results of treatment, and the detection of recurrences [48]. GCTs are divided into two main histopathological subtypes: adult and juvenile, on the basis of women's age and histological features [49]. Thus, at the histological level, the diagnosis of GCTs poses a problem in many cases. The value of mAb 12G4 as a tool for the differential diagnosis of GCTs remains to be validated, but this mAb could be useful to discriminate between GCTs and other ovarian tumours. GCTs account for 6–10 % of malignant tumours of the ovary [50] and are characterized by a tendency towards late recurrence, with a survival rate below 35 % [51]. The use of mAb 12G4 could also allow the detection of disseminated recurrences which are difficult to localize and remove. In fact, we demonstrated that mAb 12G4 detects AMHR-II not only in a primary, but also in a recurrent GCT.

Finally, mAb 12G4, with its low dissociation rate, is an attractive candidate for *in vivo* immunotargeting of AMHR-II-positive tumours, such as GCTs, Sertoli and Leydig cell tumours. GCTs, which present peritoneal carcinomatoses, are particularly well suited to immunophotodetection using fluorescent dye-labelled antibodies [52]. Furthermore, mAb 12G4 could be coupled to radionuclides for radioimmunotherapy of recurrent or metastatic tumours; particularly, small carcinomatosis tumour nodules [53,54]. The non-competitive binding of mAb 12G4 and AMH on AMHR-II should allow the use *in vivo* of mAb 12G4 in GCTs expressing a high level of AMH [47,48]. To this end, mAb 12G4 will be humanized using CDR grafting techniques.

We thank Dr N. Di Clemente for providing the CHO-3W cell line and Dr R. Cate for the gift of mAb M10.6. We thank Dr P. Durand and I. Plotton for making available the human testicular tissue. We also thank Dr Claude Granier for valuable comments and assistance with SPOT array analysis, and Dr Françoise Roquet for assistance in Biacore experiments. The authors are grateful to R. Lavaill and Dr F. Bibeau for assistance with immunohistochemical studies, and to S. Bousquié and G. Heintz for excellent technical assistance. We also thank Dr T. Chardes for a critical reading of the manuscript and Dr S. L. Salhi for presubmission editorial assistance.

REFERENCES

1 Vigier, B., Picard, J. Y., Tran, D., Legeai, L. and Josso, N. (1984) Production of anti-Mullerian hormone: another homology between Sertoli and granulosa cells. Endocrinology **114**, 1315–1320
2 Josso, N., Lamarre, I., Picard, J. Y., Berta, P., Davies, N., Morichon, N., Peschanski, M. and Jeny, R. (1993) Anti-Mullerian hormone in early human development. Early Hum. Dev. **33**, 91–99
3 Lee, M. M. and Donahoe, P. K. (1993) Mullerian inhibiting substance: a gonadal hormone with multiple functions. Endocr. Rev. **14**, 152–164
4 Jost, A., Vigier, B. and Prepin, J. (1972) Freemartins in cattle: the first steps of sexual organogenesis. J. Reprod. Fertil. **29**, 349–379
5 Behringer, R. R., Cate, R. L., Froelick, G. J., Palmiter, R. D. and Brinster, R. L. (1990) Abnormal sexual development in transgenic mice chronically expressing Mullerian inhibiting substance. Nature (London) **345**, 167–170
6 Mishina, Y., Rey, R., Finegold, M. J., Matzuk, M. M., Josso, N., Cate, R. L. and Behringer, R. R. (1996) Genetic analysis of the Mullerian-inhibiting substance signal transduction pathway in mammalian sexual differentiation. Genes Dev. **10**, 2577–2587
7 Josso, N., Racine, C., di Clemente, N., Rey, R. and Xavier, F. (1998) The role of anti-Mullerian hormone in gonadal development. Mol. Cell. Endocrinol. **145**, 3–7
8 Teixeira, J., Maheswaran, S. and Donahoe, P. K. (2001) Mullerian inhibiting substance: an instructive developmental hormone with diagnostic and possible therapeutic applications. Endocr. Rev. **22**, 657–674
9 Segev, D. L., Hoshiya, Y., Hoshiya, M., Tran, T. T., Carey, J. L., Stephen, A. E., MacLaughlin, D. T., Donahoe, P. K. and Maheswaran, S. (2002) Mullerian-inhibiting substance regulates NF-κB signaling in the prostate *in vitro* and *in vivo*. Proc. Natl. Acad. Sci. U.S.A. **99**, 239–244
10 Masiakos, P. T., MacLaughlin, D. T., Maheswaran, S., Teixeira, J., Fuller, Jr, A. F., Shah, P. C., Kehas, D. J., Kenneally, M. K., Dombkowski, D. M., Ha, T. U., Preffer, F. I. and Donahoe, P. K. (1999) Human ovarian cancer, cell lines, and primary ascites cells express the human Mullerian inhibiting substance (MIS) type II receptor, bind, and are responsive to MIS. Clin. Cancer Res. **5**, 3488–3499
11 Stephen, A. E., Masiakos, P. T., Segev, D. L., Vacanti, J. P., Donahoe, P. K. and MacLaughlin, D. T. (2001) Tissue-engineered cells producing complex recombinant proteins inhibit ovarian cancer *in vivo*. Proc. Natl. Acad. Sci. U.S.A. **98**, 3214–3219
12 Stephen, A. E., Pearsall, L. A., Christian, B. P., Donahoe, P. K., Vacanti, J. P. and MacLaughlin, D. T. (2002) Highly purified Mullerian inhibiting substance inhibits human ovarian cancer *in vivo*. Clin. Cancer Res. **8**, 2640–2646
13 Rey, R. A., Lhomme, C., Marcillac, I., Lahlou, N., Duvillard, P., Josso, N. and Bidart, J. M. (1996) Anti-Mullerian hormone as a serum marker of granulosa cell tumors of the ovary: comparative study with serum α-inhibin and estradiol. Am. J. Obstet. Gynecol. **174**, 958–965
14 Rey, R., Sabourin, J. C., Venara, M., Long, W. Q., Jaubert, F., Zeller, W. P., Duvillard, P., Chemes, H. and Bidart, J. M. (2000) Anti-Mullerian hormone is a specific marker of Sertoli- and granulosa-cell origin in gonadal tumors. Hum. Pathol. **31**, 1202–1208
15 Baarends, W. M., van Helmond, M. J., Post, M., van der Schoot, P. J., Hoogerbrugge, J. W., de Winter, J. P., Uilenbroek, J. T., Karels, B., Wilming, L. G., Meijers, J. H. et al. (1994) A novel member of the transmembrane serine/threonine kinase receptor family is specifically expressed in the gonads and in mesenchymal cells adjacent to the Mullerian duct. Development **120**, 189–197
16 di Clemente, N., Wilson, C., Faure, E., Boussin, L., Carmillo, P., Tizard, R., Picard, J. Y., Vigier, B., Josso, N. and Cate, R. (1994) Cloning, expression, and alternative splicing of the receptor for anti-Mullerian hormone. Mol. Endocrinol. **8**, 1006–1020
17 Imbeaud, S., Faure, E., Lamarre, I., Mattei, M. G., di Clemente, N., Tizard, R., Carre-Eusebe, D., Belville, C., Tragethon, L., Tonkin, C. et al. (1995) Insensitivity to anti-Mullerian hormone due to a mutation in the human anti-Mullerian hormone receptor. Nat. Genet. **11**, 382–388
18 Gouedard, L., Chen, Y. G., Thevenet, L., Racine, C., Borie, S., Lamarre, I., Josso, N., Massague, J. and di Clemente, N. (2000) Engagement of bone morphogenetic protein type IB receptor and Smad1 signaling by anti-Mullerian hormone and its type II receptor. J. Biol. Chem. **275**, 27973–27978
19 Visser, J. A., Olaso, R., Verhoef-Post, M., Kramer, P., Themmen, A. P. and Ingraham, H. A. (2001) The serine/threonine transmembrane receptor ALK2 mediates Mullerian inhibiting substance signaling. Mol. Endocrinol. **15**, 936–945
20 Jamin, S. P., Arango, N. A., Mishina, Y., Hanks, M. C. and Behringer, R. R. (2002) Requirement of Bmpr1a for Mullerian duct regression during male sexual development. Nat. Genet. **32**, 408–410
21 Clarke, T. R., Hoshiya, Y., Yi, S. E., Liu, X., Lyons, K. M. and Donahoe, P. K. (2001) Mullerian inhibiting substance signaling uses a bone morphogenetic protein (BMP)-like pathway mediated by ALK2 and induces SMAD6 expression. Mol. Endocrinol. **15**, 946–959
22 Allard, S., Adin, P., Gouedard, L., di Clemente, N., Josso, N., Orgebin-Crist, M. C., Picard, J. Y. and Xavier, F. (2000) Molecular mechanisms of hormone-mediated Mullerian duct regression: involvement of β-catenin. Development **127**, 3349–3360
23 Segev, D. L., Hoshiya, Y., Stephen, A. E., Hoshiya, M., Tran, T. T., MacLaughlin, D. T., Donahoe, P. K. and Maheswaran, S. (2001) Mullerian inhibiting substance regulates NFκB signaling and growth of mammary epithelial cells *in vivo*. J. Biol. Chem. **276**, 26799–26806
24 Tsuji, M., Shima, H., Yonemura, C. Y., Brody, J., Donahoe, P. K. and Cunha, G. R. (1992) Effect of human recombinant Mullerian inhibiting substance on isolated epithelial and mesenchymal cells during Mullerian duct regression in the rat. Endocrinology **131**, 1481–1488
25 Belville, C., Josso, N. and Picard, J. Y. (1999) Persistence of Mullerian derivatives in males. Am. J. Med. Genet. **89**, 218–223
26 Teixeira, J. and Donahoe, P. K. (1996) Molecular biology of MIS and its receptors. J. Androl. **17**, 336–341
27 Dutertre, M., Rey, R., Porteu, A., Josso, N. and Picard, J. Y. (1997) A mouse Sertoli cell line expressing anti-Mullerian hormone and its type II receptor. Mol. Cell. Endocrinol. **136**, 57–65
28 Dutertre, M., Gouedard, L., Xavier, F., Long, W. Q., di Clemente, N., Picard, J. Y. and Rey, R. (2001) Ovarian granulosa cell tumors express a functional membrane receptor for anti-Mullerian hormone in transgenic mice. Endocrinology **142**, 4040–4046
29 Racine, C., Rey, R., Forest, M. G., Louis, F., Ferre, A., Huhtaniemi, I., Josso, N. and di Clemente, N. (1998) Receptors for anti-Mullerian hormone on Leydig cells are responsible for its effects on steroidogenesis and cell differentiation. Proc. Natl. Acad. Sci. U.S.A. **95**, 594–599
30 Lee, M. M., Seah, C. C., Masiakos, P. T., Sottas, C. M., Preffer, F. I., Donahoe, P. K., Maclaughlin, D. T. and Hardy, M. P. (1999) Mullerian-inhibiting substance type II receptor expression and function in purified rat Leydig cells. Endocrinology **140**, 2819–2827

31 Baarends, W. M., Uilenbroek, J. T., Kramer, P., Hoogerbrugge, J. W., van Leeuwen, E. C., Themmen, A. P. and Grootegoed, J. A. (1995) Anti-Mullerian hormone and anti-Mullerian hormone type II receptor messenger ribonucleic acid expression in rat ovaries during postnatal development, the estrous cycle, and gonadotropin-induced follicle growth. Endocrinology **136**, 4951–4962

32 Knebelmann, B., Boussin, L., Guerrier, D., Legeai, L., Kahn, A., Josso, N. and Picard, J. Y. (1991) Anti-Mullerian hormone Bruxelles: a nonsense mutation associated with the persistent Mullerian duct syndrome. Proc. Natl. Acad. Sci. U.S.A. **88**, 3767–3771

33 Wilson, C. A., di Clemente, N., Ehrenfels, C., Pepinsky, R. B., Josso, N., Vigier, B. and Cate, R. L. (1993) Mullerian inhibiting substance requires its N-terminal domain for maintenance of biological activity, a novel finding within the transforming growth factor-β superfamily. Mol. Endocrinol. **7**, 247–257

34 Laune, D., Molina, F., Ferrieres, G., Villard, S., Bes, C., Rieunier, F., Chardes, T. and Granier, C. (2002) Application of the Spot method to the identification of peptides and amino acids from the antibody paratope that contribute to antigen binding. J. Immunol. Methods **267**, 53–70

35 Sali, A. and Blundell, T. L. (1990) Definition of general topological equivalence in protein structures. A procedure involving comparison of properties and relationships through simulated annealing and dynamic programming. J. Mol. Biol. **212**, 403–428

36 Mizuguchi, K., Deane, C. M., Blundell, T. L., Johnson, M. S. and Overington, J. P. (1998) JOY: protein sequence–structure representation and analysis. Bioinformatics **14**, 617–623

37 Sali, A. and Blundell, T. L. (1993) Comparative protein modelling by satisfaction of spatial restraints. J. Mol. Biol. **234**, 779–815

38 Sippl, M. J. (1993) Recognition of errors in three-dimensional structures of proteins. Proteins **17**, 355–362

39 Guex, N. and Peitsch, M. C. (1997) SWISS-MODEL and the Swiss-PdbViewer: an environment for comparative protein modeling. Electrophoresis **18**, 2714–2723

40 Greenwald, J., Fischer, W. H., Vale, W. W. and Choe, S. (1999) Three-finger toxin fold for the extracellular ligand-binding domain of the type II activin receptor serine kinase. Nat. Struct. Biol. **6**, 18–22

41 Hart, P. J., Deep, S., Taylor, A. B., Shu, Z., Hinck, C. S. and Hinck, A. P. (2002) Crystal structure of the human TβR2 ectodomain–TGF-β3 complex. Nat. Struct. Biol. **9**, 203–208

42 Thompson, T. B., Woodruff, T. K. and Jardetzky, T. S. (2003) Structures of an ActRIIB–activin A complex reveal a novel binding mode for TGF-β ligand–receptor interactions. EMBO J. **22**, 1555–1566

43 Greenwald, J., Groppe, J., Gray, P., Wiater, E., Kwiatkowski, W., Vale, W. and Choe, S. (2003) The BMP7/ActRII extracellular domain complex provides new insights into the cooperative nature of receptor assembly. Mol. Cell **11**, 605–617

44 Teixeira, J., Kehas, D. J., Antun, R. and Donahoe, P. K. (1999) Transcriptional regulation of the rat Mullerian inhibiting substance type II receptor in rodent Leydig cells. Proc. Natl. Acad. Sci. U.S.A. **96**, 13831–13838

45 Mendis-Handagama, S., Ariyaratne, H., Di Clemente, N. and Mrkonjich, L. (2004) Effects of luteinizing hormone and thyroid hormone on anti-Müllerian hormone receptor-type II expression in Leydig cells of prepubertal rats. Mol. Cell Endocrinol., in the press

46 Silverman, L. A. and Gitelman, S. E. (1996) Immunoreactive inhibin, Mullerian inhibitory substance, and activin as biochemical markers for juvenile granulosa cell tumors. J. Pediatr. **129**, 918–921

47 Lane, A. H., Lee, M. M., Fuller, Jr, A. F., Kehas, D. J., Donahoe, P. K. and MacLaughlin, D. T. (1999) Diagnostic utility of Mullerian inhibiting substance determination in patients with primary and recurrent granulosa cell tumors. Gynecol. Oncol. **73**, 51–55

48 Long, W. Q., Ranchin, V., Pautier, P., Belville, C., Denizot, P., Cailla, H., Lhomme, C., Picard, J. Y., Bidart, J. M. and Rey, R. (2000) Detection of minimal levels of serum anti-Mullerian hormone during follow-up of patients with ovarian granulosa cell tumor by means of a highly sensitive enzyme-linked immunosorbent assay. J. Clin. Endocrinol. Metab. **85**, 540–544

49 Scully, R. E., Young, R. H. and Clement, P. B. (1998) Sex chord-stromal tumors, granulosa tumors. In Tumors of the Ovary, Maldeveloped Gonads, Fallopian Tube, and Broad Ligament (Rosai, J., ed.), pp. 169–188, Armed Forces Institute of Pathology (AFIP), Washington

50 Fox, H., Agrawal, K. and Langley, F. A. (1975) A clinicopathologic study of 92 cases of granulosa cell tumor of the ovary with special reference to the factors influencing prognosis. Cancer **35**, 231–241

51 Pautier, P., Lhomme, C., Culine, S., Duvillard, P., Michel, G., Bidart, J. M., Gerbaulet, A. and Droz, J. P. (1997) Adult granulosa-cell tumor of the ovary: a retrospective study of 45 cases. Int. J. Gynecol. Cancer **7**, 58–65

52 Gutowski, M., Carcenac, M., Pourquier, D., Larroque, C., Rouanet, P. and Pèlegrin, A. (2001) Intraoperative immunophotodetection for radical resection of cancer: evaluation in an experimental model. Clin. Cancer Res. **7**, 1142–1148

53 Mach, J.-P., Pèlegrin, A. and Buchegger, F. (1991) Imaging and therapy with monoclonal antibodies in non-hematopoietic tumors. Curr. Opin. Immunol. **3**, 685–693

54 Chatal, J. F. and Hoefnagel, C. A. (1999) Radionuclide therapy. Lancet **354**, 931–935

Received 22 December 2003/23 January 2004; accepted 30 January 2004
Published as BJ Immediate Publication 30 January 2004, DOI 10.1042/BJ20031961